Warm α-nucleon matter

S. K. Samaddar* and J. N. De†
Saha Institute of Nuclear Physics, 1/AF Bidhannagar, Kolkata 700064, India
(Received 22 December 2010; published 9 May 2011)

The properties of warm dilute α-nucleon matter are studied in a variational approach in the Thomas-Fermi approximation starting from an effective two-body nucleon-nucleon interaction. The equation of state, symmetry energy, incompressibility of the said matter, and α fraction are in consonance with those evaluated from the virial approach, which sets the benchmark for such calculations at low densities.

DOI: 10.1103/PhysRevC.83.055802 PACS number(s): 21.65.Cd, 21.65.Ef, 21.65.Mn, 24.10.Pa

I. INTRODUCTION

Cold nuclear matter at subsaturation density as α matter has been subjected to critical study for some time [1,2]. The aim is to understand α clustering near the surface of heavy nuclei or the putative dilute α condensate in light $4n$ nuclei. In an astrophysical context, in following the evolution of core-collapse supernovas, these studies have been extended to the case of warm nuclear matter [3]. Homogeneous low-density nuclear matter stabilizes as a mixture of nucleons and nucleon clusters. It has a lower free energy than that for nucleonic matter. The cluster composition is temperature and density dependent; with increasing temperature or decreasing density, the population of heavier clusters tends to diminish, leading to a mixture of nucleons and light clusters like d, t, ^{3}He, and α [4,5]. The properties of the clusterized matter undergo a major change, for example, the incompressibility of clusterized nuclear matter is much smaller than that for homogeneous nucleon matter [6]. This directly influences the collapse and bounce phase of supernova matter. The symmetry energies of nuclear matter are also significantly affected when matter becomes clusterized [7,8]. This has an important role in a better understanding of neutrino-driven energy transfer in supernova matter [9]. The symmetry energy also influences the cluster composition in the crust of neutron stars and is thus instrumental in shaping the details of their mass, cooling, and structure [10].

The equation of state (EOS) of warm dilute nuclear matter with only light clusters up to α has recently been investigated in the virial approach [7,11]; inclusion of heavier clusters has also been made in the S-matrix (SM) framework [12]. These methods relate the calculations directly to experimental observables like the binding energies and phase shifts and, as such, are model independent. They are usually taken as *benchmark* calculations in the domain of low density and high temperature; they are understood to exhaust all the dynamical information concerning strong interactions in the medium. For an interacting quantum gas, the virial expansion, however, virtually ends at the second order. Formulation of higher order virial coefficients is very involved even at the formal level [13], making it difficult to estimate the domain of validity of the virial series truncated at the second order. It may further be noted that the density should be dilute enough so that the concept of asymptotic wave functions as being inherent in the virial expansion should be meaningful.

An alternate avenue could be to bypass the virial expansion altogether and instead use nucleation in the framework of the mean-field model with a suitably chosen effective two-nucleon interaction, which inherently takes an inclusive account of the scattering effects. Unlike the virial (SM) approach, which has direct contact with the experimental data, this method has indirect contact but it can be applied to relatively higher densities. With increasing density, a large number of different fragment species would, however, be formed, which makes the numerical calculation very lengthy. Before attempting any full-blown calculation, it may then be worthwhile, as a first step, to take only α clustering in the nuclear matter and to examine whether the model works in the low-density region where the benchmark calculations exist. The present work aims toward that end.

For study of the so-mentioned α-nucleon (αN) matter, we have chosen the Thomas-Fermi (TF) prescription for the mean-field model and the finite-range-, momentum-, and density-dependent modified Seyler-Blanchard (SBM) effective interaction [14]. The properties we explore include the EOS of the αN matter and its symmetry energy, incompressibility, α concentration, etc. In Sec. II, the theoretical framework for the mean-field and the SM approach is presented. Section III presents the results and discussion. Concluding remarks are made in Sec. IV.

II. THEORETICAL FRAMEWORK

Given an effective two-nucleon interaction, the properties of αN matter can be evaluated by exploiting the occupation functions of the n, p, and α's obtained from minimization of the thermodynamic potential of the system. In Sec. II A, some details of the effective interaction used are given. In Sec. II B, the theoretical formulation for obtaining the occupation functions from the TF approximation is presented. In Sec. II C, expressions for various observables explored are given. In Sec. II D, a brief outline of the SM approach is made.

*santosh.samaddar@saha.ac.in
†jn.de@saha.ac.in

A. The effective interaction

The form of the SBM effective interaction v is

$$v(r,\, p,\, \rho) = C_{l,u}\,[v_1(r,\, p) + v_2(r,\, \rho)]\,,$$
$$v_1 = -\left(1 - \frac{p^2}{b^2}\right) f(\mathbf{r_1}, \mathbf{r_2}), \tag{1}$$
$$v_2 = d^2\,[\rho(r_1) + \rho(r_2)]^{\kappa}\, f(\mathbf{r_1}, \mathbf{r_2}),$$

with

$$f(\mathbf{r_1}, \mathbf{r_2}) = \frac{e^{-|\mathbf{r_1}-\mathbf{r_2}|/a}}{|\mathbf{r_1} - \mathbf{r_2}|/a}. \tag{2}$$

The subscripts l and u to the interaction strength C refer to like-pair (nn or pp) and unlike-pair (np) interactions, respectively. The range of the effective interaction is given by a, and b is the measure of the strength of the momentum dependence of the interaction. The relative separation of the interacting nucleons is $\mathbf{r} = \mathbf{r_1} - \mathbf{r_2}$ and the relative momentum is $\mathbf{p} = \mathbf{p_1} - \mathbf{p_2}$; d and κ are the two parameters governing the strength of the density dependence, and $\rho(r_1)$ and $\rho(r_2)$ are the nucleon densities at the sites of the two interacting nucleons. The potential parameters are listed in Table I; the details for the determination of these parameters are given in Ref. [14]. The incompressibility K_∞ of symmetric nucleon matter is mostly governed by the parameter κ; for the potential set we have chosen, the value of $K_\infty = 238$ MeV.

The EOS of symmetric nuclear matter calculated with the SBM interaction is seen to agree extremely well [15] with that obtained in a variational approach by Friedman and Pandharipande [4] with v_{14} + TNI interaction. This interaction also reproduces quite well the binding energies, rms charge radii, charge distributions, and giant monopole resonance energies for a host of even-even nuclei ranging from ^{16}O to very heavy systems [14]. Interactions of this type has been used with great success by Myers and Swiatecki [16] in the context of nuclear mass formula.

B. Occupation functions

The self-consistent occupation probabilities of nucleons and α's in αN matter at temperature T are obtained in the TF approximation by minimizing the thermodynamic potential of the system

$$\Omega = E - TS - \sum_{\tau} \mu_\tau N_\tau - \mu_\alpha N_\alpha. \tag{3}$$

Here τ represents the isospin index (n,p). The quantities E, S, μ_τ, μ_α, N_τ, and N_α are the total internal energy, entropy, nucleon chemical potentials, α chemical potential, free nucleon number, and number of α particles, respectively,

TABLE I. Parameters of the effective interaction (in MeV fm)

C_l	C_u	a	b	d	κ
291.7	910.6	0.6199	928.2	0.879	1/6

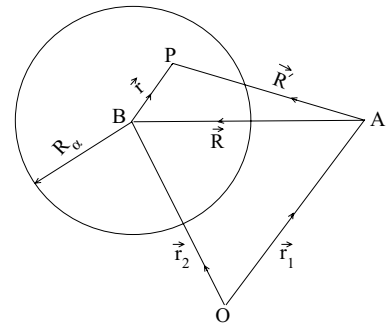

FIG. 1. Space coordinates shown for the nucleon (located at A) and α (with center at B) configuration. The origin of the coordinate system is at O and P is any arbitrary point within α.

in the system. Chemical equilibrium in the system ensures

$$\mu_\alpha = 2(\mu_n + \mu_p). \tag{4}$$

The total energy of the αN matter in the TF approximation is

$$\begin{aligned} E = \sum_\tau \Bigg\{ & \int d\mathbf{r_1} d\mathbf{p_1} \frac{p_1^2}{2m_\tau} \tilde{n}_\tau(\mathbf{p_1}) + \frac{1}{2} \int d\mathbf{r_1} d\mathbf{p_1} d\mathbf{r_2} d\mathbf{p_2} \\ & \times [v_1(|\mathbf{r_1} - \mathbf{r_2}|, |\mathbf{p_1} - \mathbf{p_2}|) + v_2(|\mathbf{r_1} - \mathbf{r_2}|, 2\rho)][C_l \tilde{n}_\tau(\mathbf{p_2}) \\ & + C_u \tilde{n}_{-\tau}(\mathbf{p_2})]\tilde{n}_\tau(\mathbf{p_1}) + \frac{1}{2}(C_l + C_u) \int d\mathbf{r_1} d\mathbf{p_1} d\mathbf{r_2} d\mathbf{p_2} \\ & \times \tilde{n}_\tau(\mathbf{p_1}) \tilde{n}_\alpha(\mathbf{p_2}) \int_{V_\alpha} d\mathbf{r} \int d\mathbf{p_i^\alpha} \tilde{n}_i^\alpha(\mathbf{p_i^\alpha}) \Bigg[v_1\big(\mathbf{R'}, \big|\mathbf{p_1} - (\mathbf{p_i^\alpha} \\ & + \mathbf{p_2})\big|\big) + v_2\Bigg(\mathbf{R'}, \Bigg(\sum_{\tau'} \rho_{\tau'} + \rho_i^\alpha\Bigg)\Bigg)\Bigg]\Bigg\} \\ & + \int d\mathbf{r_1} d\mathbf{p_1} \frac{p_1^2}{2m_\alpha} \tilde{n}_\alpha(\mathbf{p_1}) \\ & + (C_l + C_u) \int d\mathbf{r_1} d\mathbf{p_1} d\mathbf{r_2} d\mathbf{p_2} \tilde{n}_\alpha(\mathbf{p_1}) \tilde{n}_\alpha(\mathbf{p_2}) \\ & \times \int_{V_\alpha} d\mathbf{r} d\mathbf{r'} \int d\mathbf{p_i^\alpha} d\mathbf{p_i^{\alpha'}} \tilde{n}_i^\alpha(\mathbf{p_i^\alpha}) \tilde{n}_i^{\alpha'}(\mathbf{p_i^{\alpha'}}) \\ & \times \big[v_1\big(\mathbf{R'}, \big|(\mathbf{p_1} + \mathbf{p_i^\alpha}) - (\mathbf{p_2} + \mathbf{p_i^{\alpha'}})\big|\big) + v_2\big(\mathbf{R'}, 2\rho_i^\alpha\big)\big] \\ & - N_\alpha B_\alpha. \end{aligned} \tag{5}$$

In Eq. (5), m_τ and m_α are the nucleon and α masses, the first and fourth terms correspond to the kinetic energy of the nucleons and α's, the second and fifth terms refer to the interaction energy among nucleons and among α's, respectively, and the third term is the interaction energy between nucleons and α's. The various space coordinates occurring in the third and fifth terms are shown in Figs. 1 and 2, respectively.

These terms are evaluated in the single-folding and double-folding models. The last term is the binding energy contribution from the α particles. Here $\tilde{n}_\tau = \frac{2}{h^3} n_\tau$, $\tilde{n}_\alpha = \frac{1}{h^3} n_\alpha$ where n_τ and n_α are the occupation probabilities for nucleons and α's, respectively. Similarly, $\tilde{n}_i^\alpha(\mathbf{p_i^\alpha}) = \frac{2}{h^3} n_i^\alpha(\mathbf{p_i^\alpha})$ represents the occupation probability of the constituent nucleons in the α particle and $\mathbf{p_i^\alpha}$ is their intrinsic momentum inside the α. The space coordinates do not enter in the occupation functions $\tilde{n}_\tau$ and $\tilde{n}_\alpha$, as the system is infinite. For simplicity, α particles are taken to be uniform nuclear drops with a sharp surface

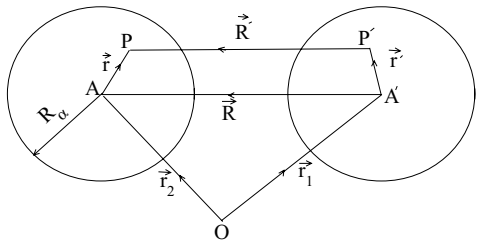

FIG. 2. Space coordinates shown for the α-α configuration with O as the origin of the coordinate system. P and P′ are arbitrary points within the α's with A and A′ as their centers.

and hence the space coordinates do not also occur in $\tilde{n}_i^\alpha$. The notation $\int_{V_\alpha}$ refers to the configuration integral over the volume of α. The integral over $\mathbf{p}_\mathbf{i}^\alpha$ is over the Fermi sphere of the nucleon momenta inside the α particles. Because α's are difficult to excite (the first excited state in α is $\sim$20 MeV), they are taken to be in their ground states. All the other integrals are over the entire configuration or momentum space unless otherwise specified. It then follows that

$$\begin{aligned}\int \tilde{n}_\tau(\mathbf{p})d\mathbf{p} &= N_\tau/V = \rho_\tau,\\ \int \tilde{n}_\alpha(\mathbf{p})d\mathbf{p} &= N_\alpha/V = \rho_\alpha,\\ \int \tilde{n}_i^\alpha(\mathbf{p})d\mathbf{p} &= 4/V_\alpha = \rho_i^\alpha,\end{aligned} \tag{6}$$

where V is the volume of the αN system and $V_\alpha = \frac{4}{3}\pi R_\alpha^3$, with R_α as the sharp-surface radius of the α drop, taken to be 2.16 fm obtained from the experimental rms charge radius of α; ρ_i^α is the density of the constituent nucleons of the α particles. The total baryon density ρ_b is given by $\rho_b = \rho + 4\rho_\alpha$, where $\rho = \sum_\tau \rho_\tau$ is the density of the free nucleons and ρ_α is the α-particle density.

The total entropy of the αN system is

$$S = \sum_\tau S_\tau + S_\alpha, \tag{7}$$

where in the Landau quasiparticle approximation,

$$\begin{aligned}S_\tau = \frac{2}{h^3}\int &[n_\tau(\mathbf{p})\ln n_\tau(\mathbf{p})\\ &+ (1-n_\tau(\mathbf{p}))\ln(1-n_\tau(\mathbf{p}))]d\mathbf{r}d\mathbf{p},\end{aligned} \tag{8}$$

and

$$\begin{aligned}S_\alpha = \frac{1}{h^3}\int &[n_\alpha(\mathbf{p})\ln n_\alpha(\mathbf{p})\\ &- (1+n_\alpha(\mathbf{p}))\ln(1+n_\alpha(\mathbf{p}))]d\mathbf{r}d\mathbf{p}.\end{aligned} \tag{9}$$

Minimization of Ω with respect to n_τ and n_α, remembering that $\delta n_\tau(\mathbf{p})$ and $\delta n_\alpha(\mathbf{p})$ are separately arbitrary over the whole phase space, at the end yields

$$\begin{aligned}&\frac{p_1^2}{2m_\tau} + \int d\mathbf{r_2}d\mathbf{p_2}\{v_1(|\mathbf{r_1}-\mathbf{r_2}|,|\mathbf{p_1}-\mathbf{p_2}|)\\ &\quad + v_2(|\mathbf{r_1}-\mathbf{r_2}|,2\rho)\}[C_l\tilde{n}_\tau(\mathbf{p_2}) + C_u\tilde{n}_{-\tau}(\mathbf{p_2})]\\ &\quad + \kappa d^2(2\rho)^{\kappa-1}\sum_{\tau'}\int d\mathbf{p_1'}d\mathbf{r_2}d\mathbf{p_2}\\ &\quad \times [C_l\tilde{n}_{\tau'}(\mathbf{p_2}) + C_u\tilde{n}_{-\tau'}(\mathbf{p_2})]\tilde{n}_{\tau'}(\mathbf{p_1}')f(\mathbf{r_1},\mathbf{r_2})\\ &\quad + \frac{1}{2}(C_l+C_u)\int d\mathbf{r_2}d\mathbf{p_2}\tilde{n}_\alpha(\mathbf{p_2})\\ &\quad \times \int d\mathbf{r}d\mathbf{p}_\mathbf{i}^\alpha\tilde{n}_i^\alpha\left(\mathbf{p}_\mathbf{i}^\alpha\right)\left\{v_1\left(\mathbf{R}',\left|\mathbf{p_1}-\left(\mathbf{p}_\mathbf{i}^\alpha+\mathbf{p_2}\right)\right|\right)\right.\\ &\quad \left. + v_2\left(\mathbf{R}',\left(\rho+\rho_i^\alpha\right)\right)\right\} + \frac{1}{4}(C_l+C_u)\kappa d^2\left(\rho+\rho_i^\alpha\right)^{\kappa-1}\\ &\quad \times \sum_{\tau'}\int d\mathbf{p_1'}d\mathbf{p_2}\tilde{n}_{\tau'}(\mathbf{p_1'})\tilde{n}_\alpha(\mathbf{p_2})\rho_i^\alpha\\ &\quad \times \int d\mathbf{r_2}\int_{V_\alpha}d\mathbf{r}\frac{e^{-|\mathbf{R}'|/a}}{|\mathbf{R}'|/a}\\ &\quad + T[\ln n_\tau(\mathbf{p_1}) - \ln(1-n_\tau(\mathbf{p_1}))] - \mu_\tau = 0\end{aligned} \tag{10}$$

and

$$\begin{aligned}&\frac{p_1^2}{2m_\alpha} + 2(C_l+C_u)\int d\mathbf{r_2}d\mathbf{p_2}\tilde{n}_\alpha(\mathbf{p_2})\\ &\quad \times \int d\mathbf{r}d\mathbf{p}_\mathbf{i}^\alpha d\mathbf{r}'d\mathbf{p}_\mathbf{i}^{\alpha\prime}\tilde{n}_i^\alpha\left(\mathbf{p}_\mathbf{i}^\alpha\right)\tilde{n}_i^{\alpha\prime}\left(\mathbf{p}_\mathbf{i}^{\alpha\prime}\right)\\ &\quad \times\left\{v_1\left(\mathbf{R}',\left|\left(\mathbf{p_1}+\mathbf{p}_\mathbf{i}^\alpha\right)-\left(\mathbf{p_2}+\mathbf{p}_\mathbf{i}^{\alpha\prime}\right)\right|\right) + v_2\left(\mathbf{R}',2\rho_i^\alpha\right)\right\}\\ &\quad + \frac{1}{2}(C_l+C_u)\sum_\tau\int d\mathbf{p_2}d\mathbf{p}_\mathbf{i}^\alpha\tilde{n}_\tau(\mathbf{p_2})\tilde{n}_i^\alpha\left(\mathbf{p}_\mathbf{i}^\alpha\right)\\ &\quad \times \int d\mathbf{r_2}\int_{V_\alpha}d\mathbf{r}\left\{v_1\left(\mathbf{R}',\left|\mathbf{p_2}-\left(\mathbf{p_1}+\mathbf{p}_\mathbf{i}^\alpha\right)\right|\right)\right.\\ &\quad \left. + v_2\left(\mathbf{R}',\rho+\rho_i^\alpha\right)\right\} + T[\ln n_\alpha(\mathbf{p_1}) - \ln(1+n_\alpha(\mathbf{p_1}))]\\ &\quad - (\mu_\alpha + B_\alpha) = 0.\end{aligned} \tag{11}$$

Without any loss of generality, $\mathbf{r_1}$ can be set equal to 0 in Eqs. (10) and (11). The single-particle occupation functions $n_\tau(p)$ and $n_\alpha(p)$ for nucleons and α's are determined from Eqs. (10) and (11), respectively. Equation (10), after some algebraic manipulations, can be written as

$$\begin{aligned}&\frac{p_1^2}{2m_\tau} + V_\tau^0 + p_1^2V_\tau^1 + V_\tau^2\\ &\quad + T[\ln n_\tau(\mathbf{p_1}) - \ln(1-n_\tau(\mathbf{p_1}))] - \mu_\tau = 0.\end{aligned} \tag{12}$$

The momentum-dependent nucleon single-particle potential $V_\tau(p)$ is given by

$$V_\tau(p) = V_\tau^0 + p^2V_\tau^1, \tag{13}$$

where V_τ^0 is the momentum-independent part. Equation (12) leads to

$$n_\tau(p) = \left[1+\exp\left\{\left(\frac{p^2}{2m_\tau^*} + V_\tau^0 + V_\tau^2 - \mu_\tau\right)/T\right\}\right]^{-1}, \tag{14}$$

where m_τ^* is the nucleon effective mass,

$$m_\tau^* = \left[\frac{1}{m_\tau} + 2V_\tau^1\right]^{-1}, \tag{15}$$

and V_τ^2 is the rearrangement potential coming from the density dependence of the interaction. Similarly Eq. (11) can be written

as

$$\frac{p_1^2}{2m_\alpha} + V_\alpha^0 + p_1^2 V_\alpha^1 + T[\ln n_\alpha(\mathbf{p_1}) - \ln(1 + n_\alpha(\mathbf{p_1}))] - (\mu_\alpha + B_\alpha) = 0, \tag{16}$$

which yields

$$n_\alpha(p) = \left[\exp\left(\left\{\frac{p^2}{2m_\alpha^*} + V_\alpha^0 - (\mu_\alpha + B_\alpha)\right\}/T\right) - 1\right]^{-1}, \tag{17}$$

where

$$m_\alpha^* = \left[\frac{1}{m_\alpha} + 2V_\alpha^1\right]^{-1} \tag{18}$$

is the α effective mass. V_α^0 is the momentum-independent part of the α single particle potential $V_\alpha (= V_\alpha^0 + p^2 V_\alpha^1)$ in the system. The nucleon and α masses are renormalized owing to the momentum dependence of the interaction.

The expressions for V_τ^0 can be arrived at as

$$V_\tau^0 = -4\pi a^3\{1 - d^2(2\rho)^\kappa\}(C_l\rho_\tau + C_u\rho_{-\tau}) + \frac{16\pi^2 a^3}{b^2 h^3}[C_l(2m_\tau^* T)^{5/2} J_{3/2}(\eta_\tau) + C_u(2m_{-\tau}^* T)^{5/2} \times J_{3/2}(\eta_{-\tau})] + \frac{1}{4} I(C_l + C_u)\rho_\alpha \rho_\alpha^i \left[\frac{\langle p_\alpha^2\rangle + \langle (p_i^\alpha)^2\rangle}{b^2} + d^2\left(\rho + \rho_i^\alpha\right)^\kappa - 1\right]. \tag{19}$$

The first two terms come from the interaction between free nucleons; the last term originates from the presence of α's. In Eq. (19), I is the six-dimensional integral (see Fig. 1)

$$I = \int_{V_\alpha} d\mathbf{r} \int d\mathbf{R} \frac{e^{-|\mathbf{r}+\mathbf{R}|/a}}{|\mathbf{r}+\mathbf{R}|/a}. \tag{20}$$

This integral can be evaluated analytically. The quantity $\langle p_\alpha^2\rangle$ is the mean squared value of the α momentum in αN matter and $\langle (p_i^\alpha)^2\rangle$ is the mean squared value of the constituent nucleon momentum inside the α. The value of $\langle p_\alpha^2\rangle$ is

$$\langle p_\alpha^2\rangle = (2m_\alpha^* T) B_{3/2}(\eta_\alpha)/B_{1/2}(\eta_\alpha) \simeq 3m_\alpha^* T, \tag{21}$$

and

$$\langle (p_i^\alpha)^2\rangle \simeq \frac{3}{5}\left(P_F^\alpha\right)^2, \tag{22}$$

where P_F^α is the value of the zero-temperature nucleon Fermi momentum inside α, taken to be 220.5 MeV/c, consistent with the α sharp surface radius. The $J_k(\eta)$ and $B_k(\eta)$ are the Fermi and Bose integrals,

$$J_k(\eta) = \int_0^\infty \frac{x^k dx}{e^{(x-\eta)} + 1} \tag{23}$$

and

$$B_k(\eta) = \int_0^\infty \frac{x^k dx}{e^{(x-\eta)} - 1}, \tag{24}$$

with

$$\eta_\tau = \left(\mu_\tau - V_\tau^0 - V_\tau^2\right)/T, \quad \eta_\alpha = \left(\mu_\alpha + B_\alpha - V_\alpha^0\right)/T. \tag{25}$$

The expressions for V_τ^1, V_τ^2, V_α^0, and V_α^1 are given as

$$V_\tau^1 = \frac{4\pi a^3}{b^2}[C_l\rho_\tau + C_u\rho_{-\tau}] + \frac{1}{4} I(C_l + C_u)\frac{\rho_\alpha \rho_\alpha^i}{b^2}, \tag{26}$$

$$V_\tau^2 = 4\pi a^3 \kappa d^2 (2\rho)^{\kappa-1} \sum_{\tau'}[C_l\rho_{\tau'} + C_u\rho_{-\tau'}]\rho_{\tau'} + \frac{1}{4} I(C_l + C_u)\kappa d^2\left(\rho + \rho_i^\alpha\right)^{\kappa-1}\rho_i^\alpha \rho_\alpha \rho, \tag{27}$$

$$V_\alpha^0 = \frac{1}{4}(C_l + C_u)\rho_i^\alpha \left\{2\rho_i^\alpha \rho_\alpha I_\alpha \left[d^2\left(2\rho_i^\alpha\right)^\kappa - 1 + \frac{3m_\alpha^* T + \frac{6}{5}\left(P_F^\alpha\right)^2}{b^2}\right] + I\left[\rho\left\{d^2\left(\rho + \rho_i^\alpha\right)^\kappa - 1 + \frac{3}{5}\frac{\left(P_F^\alpha\right)^2}{b^2}\right\} + \sum_\tau \frac{4\pi(2m_\tau^* T)^{5/2} J_{3/2}(\eta_\tau)}{h^3 b^2}\right]\right\} \tag{28}$$

and

$$V_\alpha^1 = \tfrac{1}{4}(C_l + C_u)\rho_i^\alpha\left\{2\rho_i^\alpha \rho_\alpha I_\alpha + I\rho\right\}/b^2. \tag{29}$$

In both V_τ^1 and V_τ^2, the last term stems from the α-N interaction. The effective nucleon mass in pure nucleonic matter thus gets modified owing to clusterization. The integral I_α occurring in Eqs. (28) and (29) is a nine-dimensional integral (see Fig. 2),

$$I_\alpha = \int_{V_\alpha} d\mathbf{r} \int_{V_\alpha} d\mathbf{r}' \int d\mathbf{R} \frac{e^{-|\mathbf{R}+\mathbf{r}-\mathbf{r}'|/a}}{|\mathbf{R}+\mathbf{r}-\mathbf{r}'|/a}, \tag{30}$$

which can be evaluated numerically. If the α's do not interpenetrate, the integral over $\mathbf{R}$ excludes the α volumes.

C. Expressions for observables in the TF approximation

1. Energy per baryon

The energy per baryon e_b of the αN matter can be calculated from Eq. (5). It can be split into the following form:

$$e_b = e_{NN} + e_{\alpha N} + e_{\alpha\alpha}. \tag{31}$$

Here e_{NN} comes from the kinetic energy of the free nucleons and the interactions among them, $e_{\alpha N}$ arises from the interaction among the free nucleons and the α's, and $e_{\alpha\alpha}$ stems from the kinetic energy of the α's and the interaction among themselves. The expressions for them are

$$e_{NN} = \frac{1}{\rho_b}\sum_\tau \rho_\tau \left[T J_{3/2}(\eta_\tau)/J_{1/2}(\eta_\tau)\left\{1 - m_\tau^* V_\tau^1\right\} + \frac{1}{2}V_\tau^0\right], \tag{32}$$

$$e_{\alpha N} = \frac{1}{4\rho_b}(C_l + C_u) I \rho_\alpha \rho_\alpha^i \left[\left\{\frac{3m_\alpha^* T + 3/5\left(P_F^\alpha\right)^2}{b^2} - 1 + d^2\left(\rho + \rho_i^\alpha\right)^\kappa\right\}\rho + \frac{1}{b^2}\sum_\tau\left(\frac{4\pi}{h^3}(2m_\tau^* T)^{5/2} J_{3/2}(\eta_\tau)\right)\right] \tag{33}$$

and

$$e_{\alpha\alpha} = \frac{1}{\rho_b}\Bigg[\frac{\pi}{m_\alpha h^3}(2m_\alpha^* T)^{5/2} B_{3/2}(\eta_\alpha) + \frac{1}{4}(C_l + C_u) I_\alpha \rho_\alpha^2 (\rho_i^\alpha)^2 \Bigg\{ d^2 (2\rho_i^\alpha)^\kappa - 1 + \frac{6m_\alpha^* T}{b^2} + \frac{6}{5}\frac{(P_F^\alpha)^2}{b^2} \Bigg\}\Bigg]. \tag{34}$$

In the above equations, as stated earlier, ρ_b $(=\rho + 4\rho_\alpha)$ corresponds to the total baryon density, and ρ and ρ_α are the free nucleon and α densities, respectively, in the αN system.

2. Entropy per baryon

The entropy per baryon s_b can be evaluated using Eqs. (8) and (9). It is additive and can be written as

$$s_b = s_N + s_\alpha, \tag{35}$$

where s_N and s_α are the contributions to entropy from free nucleons and α's, respectively. Their expressions reduce to

$$s_N = \frac{1}{\rho_b}\sum_\tau \rho_\tau \left[\frac{5}{3} J_{3/2}(\eta_\tau)/J_{1/2}(\eta_\tau) - \eta_\tau\right] \tag{36}$$

and

$$s_\alpha = \frac{\rho_\alpha}{\rho_b}\left[\frac{5}{3} B_{3/2}(\eta_\alpha)/B_{1/2}(\eta_\alpha) - \eta_\alpha\right]. \tag{37}$$

3. Pressure of αN matter

Once the energy and entropy of the composite system are known, the pressure can be calculated from the Gibbs-Duhem thermodynamic identity,

$$P = \sum_\tau \rho_\tau \mu_\tau + \rho_\alpha \mu_\alpha - f_b \rho_b, \tag{38}$$

where f_b is the free energy per baryon, $f_b = e_b - T s_b$.

4. Incompressibility and symmetry coefficients

The incompressibility K can be computed from the derivative of pressure

$$K = 9\frac{dP}{d\rho}. \tag{39}$$

The symmetry free energy and symmetry energy coefficients C_F and C_E are calculated from

$$C_F = \frac{1}{2}\left(\frac{\partial^2 f_b}{\partial X^2}\right)_{X=0}, \tag{40}$$

$$C_E = \frac{1}{2}\left(\frac{\partial^2 e_b}{\partial X^2}\right)_{X=0}, \tag{41}$$

where X is the neutron-proton asymmetry of the αN system. It is given as $X = (\rho_b^n - \rho_b^p)/\rho_b$, where ρ_b^n and ρ_b^p are the total neutron and proton density, respectively.

D. The *S*-matrix approach

The relevant key elements of the SM framework [17] as applied in the context of dilute nuclear matter [8,12] are outlined in brief here. The grand partition function of an interacting infinite system of neutrons and protons can be written as

$$\mathcal{Z} = \sum_{Z,N=0}^{\infty} (\zeta_p)^Z (\zeta_n)^N \,\mathrm{Tr}_{Z,N}\, e^{-\beta H}, \tag{42}$$

where $\zeta_p = e^{\beta\mu_p}$ and $\zeta_n = e^{\beta\mu_n}$ are the elementary fugacities with $\beta = 1/T$, and μ's are the nucleonic chemical potentials. Here H is the total Hamiltonian of the system and the trace $\mathrm{Tr}_{Z,N}$ is taken over states of Z protons and N neutrons. The partition function can be split into two types of terms [17]:

$$\ln \mathcal{Z} = \ln \mathcal{Z}_{\mathrm{part}}^{(0)} + \ln \mathcal{Z}_{\mathrm{scat}}. \tag{43}$$

The first term on the right-hand side corresponds to contributions from stable single-particle states of clusters of different sizes including free nucleons formed in the system; the second term refers to all possible scattering states. The superscript (0) indicates that the clusters behave as an ideal quantum gas. In general, $\ln \mathcal{Z}_{\mathrm{part}}^{(0)}$ contains contributions from the ground states as well as the particle-stable excited states of all the clusters. The scattering term $\ln \mathcal{Z}_{\mathrm{scat}}$ may be written as a sum of scattering contributions from a set of channels, each set having total proton number Z_t and neutron number N_t. Because our interest in the present work is focused on αN matter, in $\ln \mathcal{Z}_{\mathrm{part}}^{(0)}$, we include only the nucleons and the ground state of α; similarly in $\ln \mathcal{Z}_{\mathrm{scat}}$, only the scattering channels NN, αN, and $\alpha\alpha$ are considered, so that

$$\ln \mathcal{Z}_{\mathrm{scat}} = \ln \mathcal{Z}_{NN} + \ln \mathcal{Z}_{\alpha N} + \ln \mathcal{Z}_{\alpha\alpha}. \tag{44}$$

Each of the terms in Eq. (44) can be expanded in the respective virial coefficients. Only expansion up to the second-order coefficients is considered. They are written as energy integrals of the relevant phase shifts [6,7]. The partition function can then be written explicitly as

$$\ln \mathcal{Z} = V\Bigg\{\frac{2}{\lambda_N^3}\Bigg[\zeta_n + \zeta_p + \frac{b_{nn}}{2}\zeta_n^2 + \frac{b_{pp}}{2}\zeta_p^2 + \frac{1}{2}b_{np}\zeta_n\zeta_p + 8\zeta_\alpha + 8b_{\alpha\alpha}\zeta_\alpha^2 + 8b_{\alpha n}\zeta_\alpha(\zeta_n + \zeta_p)\Bigg]\Bigg\}, \tag{45}$$

where $\lambda_N = \frac{h}{\sqrt{2\pi m T}}$ is the nucleon thermal wavelength, $\zeta_\alpha = e^{\beta(\mu_\alpha + B_\alpha)}$, B_α being the binding energy of α and $\mu_\alpha = 2(\mu_n + \mu_p)$. b_{nn}, b_{np}, etc., are the temperature-dependent virial coefficients [7,12]. The value of the virial coefficient b_{np} has been adjusted so as to exclude the resonance formation of deuteron from n-p scattering to be consistent with our choice of the αN matter.

Knowledge of the partition function allows all the relevant observables to be calculated. The pressure is given by

$$P = T \ln \mathcal{Z}/V. \tag{46}$$

The number density ρ_i is calculated from

$$\rho_i = \zeta_i \left(\frac{\partial}{\partial \zeta_i}\frac{\ln \mathcal{Z}}{V}\right)_{V,T}, \tag{47}$$

where i stands for n, p, or α. Once the pressure, densities, and chemical potentials are known, the free energy can be obtained from the Gibbs-Duhem relation. The entropy per baryon is calculated from

$$s_b = \frac{1}{\rho_b}\left(\frac{\partial P}{\partial T}\right)_\mu, \tag{48}$$

which yields the energy per baryon as $e_b = f_b + T s_b$. The explicit expression for the entropy per baryon is

$$s_b = \frac{1}{\rho_b}\left\{\frac{5}{2}\frac{P}{T} - \sum_i \rho_i \ln \zeta_i + \frac{T}{\lambda_N^3}\left[\zeta_n\zeta_p b'_{np} + \left(\zeta_n^2 + \zeta_p^2\right)b'_{nn} + 8\zeta_\alpha^2 b'_{\alpha\alpha} + 8\zeta_\alpha(\zeta_n + \zeta_p)b'_{\alpha n}\right]\right\}. \tag{49}$$

The prime on the virial coefficients denotes their temperature derivatives.

III. RESULTS AND DISCUSSION

In the mean-field framework, the momentum- and density-dependent finite-range SBM force as scripted in Eqs. (1) and (2) has been chosen as the effective two-nucleon interaction in our calculations. To start with, we take baryon matter at a given density ρ_b at a temperature T with an isospin asymmetry X. The unknowns are the free nucleon densities ρ_n, ρ_p and the α concentration in the matter. The three constraints are the conservation of the total baryon number, the total isospin, and the condition of chemical equilibrium between the nucleons and the α's. Starting from a guess value for the α concentration, the unknowns are determined iteratively using the Newton-Raphson method. For our calculations, the masses of neutron and proton are taken to be the same, and for α binding energy, the experimental value of 28.3 MeV is used. For evaluation of the $\alpha\alpha$ potential, the α-particles are assumed to be nuclear droplets with sharp boundaries that do not interpenetrate.

The calculations are done up to a baryon density $\rho_b = 0.01$ fm^{-3}. To show the effect of temperature on different properties of the dilute matter, results are reported for temperatures $T = 3, 5$, and 10 MeV. The baryon fraction in α, $Y_\alpha = 4\rho_\alpha/\rho_b$ (hereafter referred to as the α fraction) in αN matter as a function of density at the three temperatures mentioned are shown for symmetric ($X = 0$) and asymmetric ($X = 0.2$) nuclear matter in Figs. 3(a) and 3(b), respectively. Black lines correspond to results obtained in the TF approximation [αN (TF)]; red lines refer to those in the SM approach [αN (SM)], with consideration of only n, p, and α as the constituents of the baryonic matter. At low temperatures and higher densities, it is seen that α's are the major constituents of the matter; with increasing temperature, the free nucleon fraction increases at the cost of α density. At moderate asymmetry $X = 0.2$, the α population is somewhat lower compared to that for symmetric nuclear matter. In the temperature and density domain that we explore, the results from both the SM and the TF approach are found to be quite close. The asymmetry dependence of α fraction Y_α is displayed in Fig. 4 at two representative densities, $\rho_b = 0.001$ and 0.01 fm^{-3}, at the three temperatures.

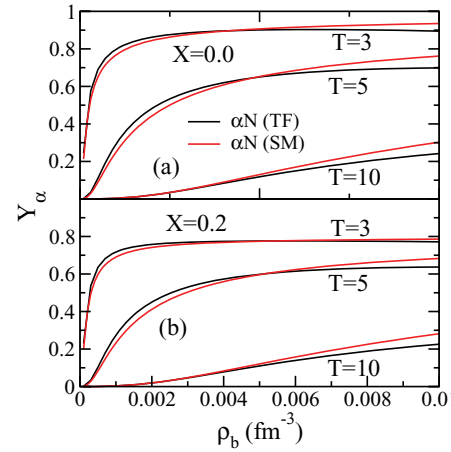

FIG. 3. (Color online) The α fraction $Y_\alpha = 4\rho_\alpha/\rho_b$ shown as a function of the baryon density ρ_b in the TF and SM approaches at $T = 3$, 5, and 10 MeV for symmetric matter ($X = 0.0$) and asymmetric matter ($X = 0.2$) in (a) and (b), respectively.

With increasing asymmetry, the α concentration decreases; the decrease is more prominent at lower temperature. At the lower density [Fig. 4(a)], results for $T = 10$ MeV are not shown, as Y_α is close to 0.

The free energy per baryon for homogeneous nucleonic matter [denoted N(TF)] and the αN matter in the TF approximation are presented in Figs. 5(a), 5(b), and 5(c) at $T = 3$, 5, and 10 MeV, respectively. The calculations presented refer to symmetric nuclear matter. Blue and black lines represent results for N(TF) and αN(TF). It is clearly shown that the clusterized matter has a lower free energy compared to the homogeneous nucleonic matter. This is more prominent at lower temperatures; higher temperatures tend to melt away the clusters. For comparison, results from the SM approach are also presented. They are shown by the red lines, nearly indistinguishable from those for αN(TF). Figure 6 displays the pressure of the baryonic matter. At lower temperatures ($T = 3$ and 5 MeV), the nucleonic matter

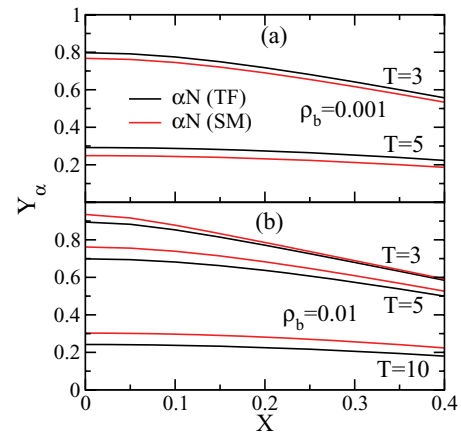

FIG. 4. (Color online) The α fraction Y_α displayed as a function of asymmetry X at baryon density $\rho_b = 0.001$ (top) and at 0.01 fm^{-3} (bottom) at $T = 3$, 5, and 10 MeV in the TF and SM approaches.

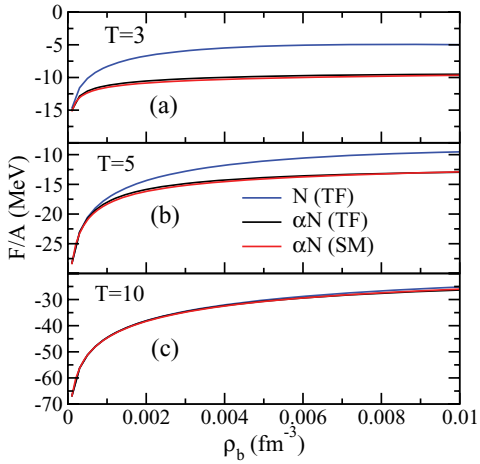

FIG. 5. (Color online) Free energy per baryon F/A shown as a function of ρ_b at $T = 3$, 5, and 10 MeV in the TF framework for homogeneous nucleonic matter (blue lines) and αN matter (black lines). Red lines represent results from the SM approach.

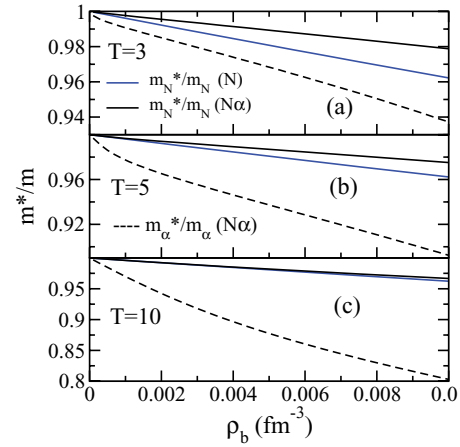

FIG. 7. (Color online) The nucleon (solid black lines) and α (dashed black lines) effective masses shown as a function of ρ_b at $T = 3$, 5, and 10 MeV in the TF framework for αN matter. Blue lines refer to the corresponding nucleon effective masses for homogeneous nucleonic matter.

shows the rise and fall of the pressure with density leading to an unphysical region. For αN matter, however, no such unphysical region is observed in the density region we have studied. Both the TF and the SM approaches yield nearly the same value of pressure. At high temperatures the α concentration becomes very much lower; the pressure in all three approaches are then nearly the same in this density region.

In Fig. 7, effective masses of the nucleon and α are shown as a function of density at the temperatures mentioned. The nucleon effective mass is calculated for both nucleonic matter (blue line) and αN matter (solid black line) in the TF approximation. The nucleon effective mass at a given ρ_b in homogeneous nucleonic matter is always lower compared to that in clusterized matter. It is independent of temperature. In αN matter it nominally decreases with temperature. At high temperatures, the nucleon effective masses calculated in the homogeneous and clusterized matter are nearly degenerate; with lowering of temperature, the degeneracy is lifted owing to the increase in α concentration. The effective α mass is shown by the dashed black lines. With increasing temperature, the medium effect on the α mass is strikingly enhanced. This is because of the interplay of the temperature-dependent contributions from the $\alpha\alpha$ interactions and αN interactions, corresponding to the first and the second term within the braces in Eq. (29).

The incompressibility of the baryonic matter as a function of density is displayed in Fig. 8 at the three temperatures. At a very low density and higher temperature, the matter is mostly nucleonic in all three approaches, so the incompressibility K is $\sim 9T$; one sees this at the lower densities considered at $T =$ 10 MeV in Fig. 8(c). Even at this very high temperature, however, the nucleonic interactions have their role as the density increases; this results in the reduction of the incompressibility from the ideal gas value. At the lower temperatures [Figs. 8(a)

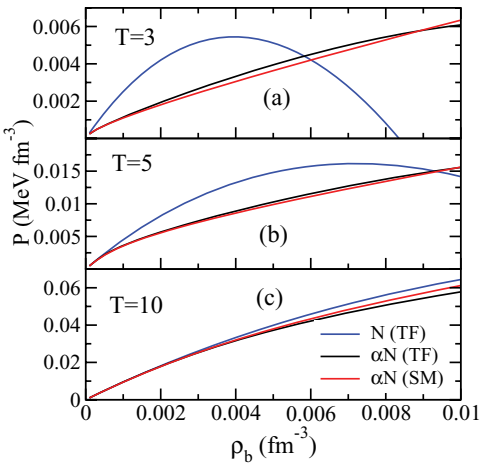

FIG. 6. (Color online) Pressure P as a function of ρ_b. Notation is the same as in Fig. 5.

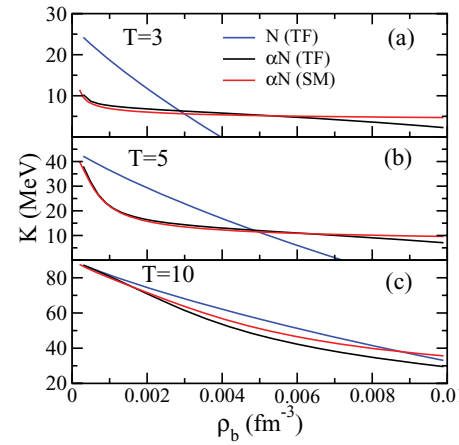

FIG. 8. (Color online) Incompressibility K for baryonic matter shown as a function of ρ_b at $T = 3$, 5, and 10 MeV. Notation is the same as in Fig. 5.

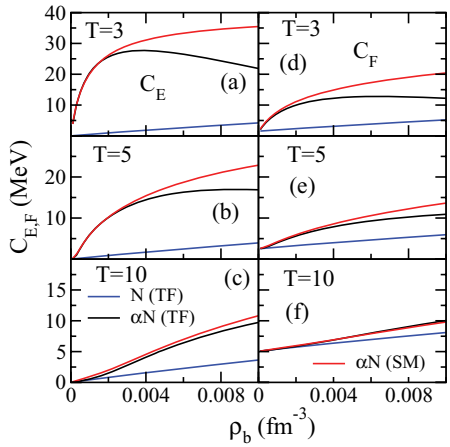

FIG. 9. (Color online) Symmetry energy C_E (left) and symmetry free energy coefficients C_F (right) shown as a function of ρ_b at temperatures $T = 3$, 5, and 10 MeV. Notation is the same as in Fig. 5.

and 8(b)], clusterization softens the matter toward compression compared to homogeneous matter (shown in the lower density region); increasing density, however, pushes the homogeneous matter toward the unphysical region, leading to negative incompressibility.

The symmetry energy coefficients C_E and C_F of the baryonic matter as a function of density are displayed in the left and right panels, respectively, of Fig. 9 at the three temperatures studied. Blue lines refer to calculations for the homogeneous matter; black and red lines represent results for αN(TF) and αN(SM). Clusterized matter displays a marked increase in the symmetry coefficients, noticed earlier [6,7]. The two approaches to clusterization lead to the same values of the symmetry coefficients at lower densities; with an increase in density the difference widens, more so at lower temperatures.

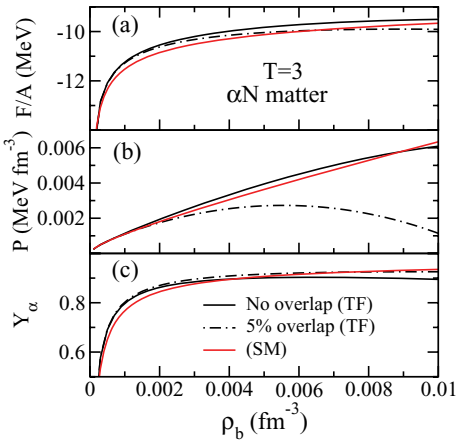

FIG. 10. (Color online) (a) Free energy per particle, (b) pressure, and (c) α fraction shown as a function of ρ_b at $T = 3$ MeV for α drops with no overlap (solid black lines) and with, at best, 5% overlap (dashed-dotted black lines) in the TF approximation. The same observables are also shown in the SM approach (red lines).

The results presented so far in the αN(TF) approach have been calculated with the assumption that the α's do not overlap; they are mutually impenetrable spherical drops. This assumption relies on the fact that the α's are very tightly bound and very hard to excite. To explore the effect of overlap in α's, we consider the possibility of penetration with, at best, a 5% overlap in volume [the value of I_α in Eq. (30) then changes accordingly]. Calculations have been repeated with this changed condition. The so-calculated free energy per baryon, pressure, and α fraction Y_α in the baryonic matter are presented in Figs. 10(a), 10(b), and 10(c), respectively, at $T = 3$ MeV (the dot-dashed black lines) and compared with those calculated with the no-overlap condition (solid black lines) and also those from the αN(SM) approach (red lines). There is no significant change in the free energy or in the α fraction, but the pressure changes perceptibly, particularly at higher densities. The good agreement between the no-overlap αN(TF) calculations and those from the benchmark αN(SM) shows the viability of the approximation of the impenetrability of the α's.

IV. CONCLUDING REMARKS

Clusterization in warm dilute nuclear matter has been treated earlier in the virial approach or in the SM framework. These are model-independent parameter-free calculations. As explained in Sec. I, these methods may have limitations at relatively high densities and low temperatures. An alternate avenue for dealing with clusterized matter in a broadened density and temperature domain is suggested in the mean-field framework in the present paper. The suggested method may be lengthy at relatively higher densities where many different fragment species are formed, but it is straightforward. To explore its applicability in a wider domain, as a first step, we consider only n, p, and α as the constituents of the matter at low densities and see how the results compare with those from the model-independent virial approach.

We have chosen the SBM interaction, which nicely reproduces the bulk properties of nuclear matter and of finite nuclei. We have calculated the α fraction, free energy, pressure, incompressibility, and symmetry coefficients of this αN matter in this mean-field framework and find that all these results compare extremely well with those obtained from the SM method, particularly in the low-density, high-temperature regime. This gives one confidence in the applicability of this mean-field approach in dealing with the EOS of warm dilute baryonic matter and the possibility of extending this method to higher densities. The price, however, is the consideration of a larger number of fragment species and a numerically involved calculation.

ACKNOWLEDGMENTS

S.K.S. and J.N.D acknowledge support from the DST, Government of India.

[1] J. W. Clark and T. P. Wang, Ann. Phys. (NY) **40**, 127 (1966).
[2] F. Carstoiu and S. Misicu, Phys. Lett. B **682**, 33 (2009).
[3] D. Q. Lamb, J. M. Lattimer, C. J. Pethick, and D. G. Ravenhall, Phys. Rev. Lett. **41**, 1623 (1978).
[4] B. Friedman and V. R. Pandharipande, Nucl. Phys. A **361**, 502 (1981).
[5] G. Peilert, J. Randrup, H. Stocker, and W. Greiner, Phys. Lett. B **260**, 271 (1991).
[6] S. K. Samaddar, J. N. De, X. Viñas, and M. Centelles, Phys. Rev. C **80**, 035803 (2009).
[7] C. J. Horowitz and A. Schwenk, Nucl. Phys. A **776**, 55 (2006).
[8] J. N. De, S. K. Samaddar, and B. K. Agrawal, Phys. Rev. C **82**, 045201 (2010).
[9] H.-Th. Janka, K. Langanke, A. Marek, G. Martínez-Pinedo, and B. Müller, Phys. Rep. **442**, 38 (2007).
[10] C. Fuchs, J. Phys. G **35**, 014049 (2008).
[11] E. O'Connor, D. Gazit, C. J. Horowitz, A. Schwenk, and N. Barnea, Phys. Rev. C **75**, 055803 (2007).
[12] S. Mallik, J. N. De, S. K. Samaddar, and Sourav Sarkar, Phys. Rev. C **77**, 032201(R) (2008).
[13] A. Pais and G. E. Uhlenbeck, Phys. Rev. **116**, 250 (1959).
[14] J. N. De, N. Rudra, Subrata Pal, and S. K. Samaddar, Phys. Rev. C **53**, 780 (1996).
[15] V. S. Uma Maheswari, D. N. Basu, J. N. De, and S. K. Samaddar, Nucl. Phys. A **615**, 516 (1997).
[16] W. D. Myers and W. J. Swiatecki, Ann. Phys. (NY) **204**, 401 (1990).
[17] R. Dashen, S-k. Ma, and H. J. Bernstein, Phys. Rev. **187**, 345 (1969).